REVIEW

On-surface synthesis and atomic scale characterization of unprotected indenofluorene polymers

Marco Di Giovannantonio[1] ⓘ | **Roman Fasel**[1,2] ⓘ

[1]Empa, Swiss Federal Laboratories for Materials Science and Technology, nanotech@surfaces Laboratory, Dübendorf, Switzerland

[2]Department of Chemistry, Biochemistry and Pharmaceutical Sciences, University of Bern, Bern, Switzerland

Correspondence
Marco Di Giovannantonio, Istituto di Struttura della Materia – CNR (ISM-CNR), Rome, Italy.
Email: marco.digiovannantonio@ism.cnr.it

Present address
Marco Di Giovannantonio, Istituto di Struttura della Materia - CNR (ISM-CNR), Rome, Italy

Funding information
Swiss National Science Foundation, Grant/Award Number: 200020_182015

Abstract

Polycyclic hydrocarbons with nonzero radical character have attracted enormous interest as potential active media for organic electronics and spintronics. In this context, indenofluorenes are an intriguing class of formally antiaromatic, biradical materials with a radical character that depends on the connectivity of their six- and five-membered rings. Synthesis of indenofluorene polymers and related compounds, first achieved in the early '90s with the production of ladder-type chains, represents a major step toward incorporation of these systems into devices. However, solution-based synthetic protocols require bulky protecting groups to stabilize the most reactive sites and, at the same time, to improve solubility and processability of such compounds. The preparation of various pristine – that is, unprotected—indenofluorene polymers has recently become possible via the on-surface synthesis approach, where the resulting nanostructures are supported and efficiently stabilized by the underlying substrate in ultrahigh vacuum conditions. Here, an overview of these recent works is given, with a focus on synthetic challenges, structural details and electronic properties.

KEYWORDS
indenofluorenes, methyl groups, nc-AFM, on-surface synthesis, polymers, STM/STS

1 | INTRODUCTION

Indenofluorenes (IFs) are non-alternant, non-benzenoid polycyclic hydrocarbons (PCHs) made of a conjugated array of fused 6–5–6–5–6-membered rings. They have attracted interest in virtue of narrow energy gaps, open-shell biradical character, and—due to the presence of 20 π-electrons in their scaffold—formal antiaromaticity.[1–5] Open-shell molecules are systems that display unpaired electrons, usually unstable and observed as short-lived intermediates during chemical reactions. In general, the electronic structures of these compounds are described by the quantum chemical biradical character index, referred to as y. Formally, y can be expressed as $y = 1 - (2\,T/[1 + T^2])$, where T takes into account the occupation number (n) of the highest occupied and lowest unoccupied natural orbitals: $T = (n_{HONO} - n_{LUNO})/2$.[4] Five IF regioisomers exist, where the six- and five-membered rings are differently connected together ($I–V$ in Scheme 1A). All these compounds exhibit resonant electronic structures between open- and closed-shell configurations, with values of y that cover almost the entire range from 0 to 1, where 0 and

---

Dedicated to Professor Klaus Müllen on the occasion of his 75th birthday.

SCHEME 1 IFs and IF polymers. (A) Resonance structures of the five IF regioisomers (*I-V*), with ground state electronic configurations and biradical character indices (*y*), obtained from Fukuda et al.[6] and Di Giovannantonio et al.[7] at the LC-UBYLP/6-311+G** level of theory. Clar sextets are highlighted in blue. Reproduced with permission.[7] Copyright 2019, American Chemical Society. (B) Molecular precursors used to grow IF polymers on surfaces, and the resulting products. STS-measured band gaps of the polymers adsorbed on Au(111) are reported next to the structures, and range from 0.4 eV to 2.3 eV
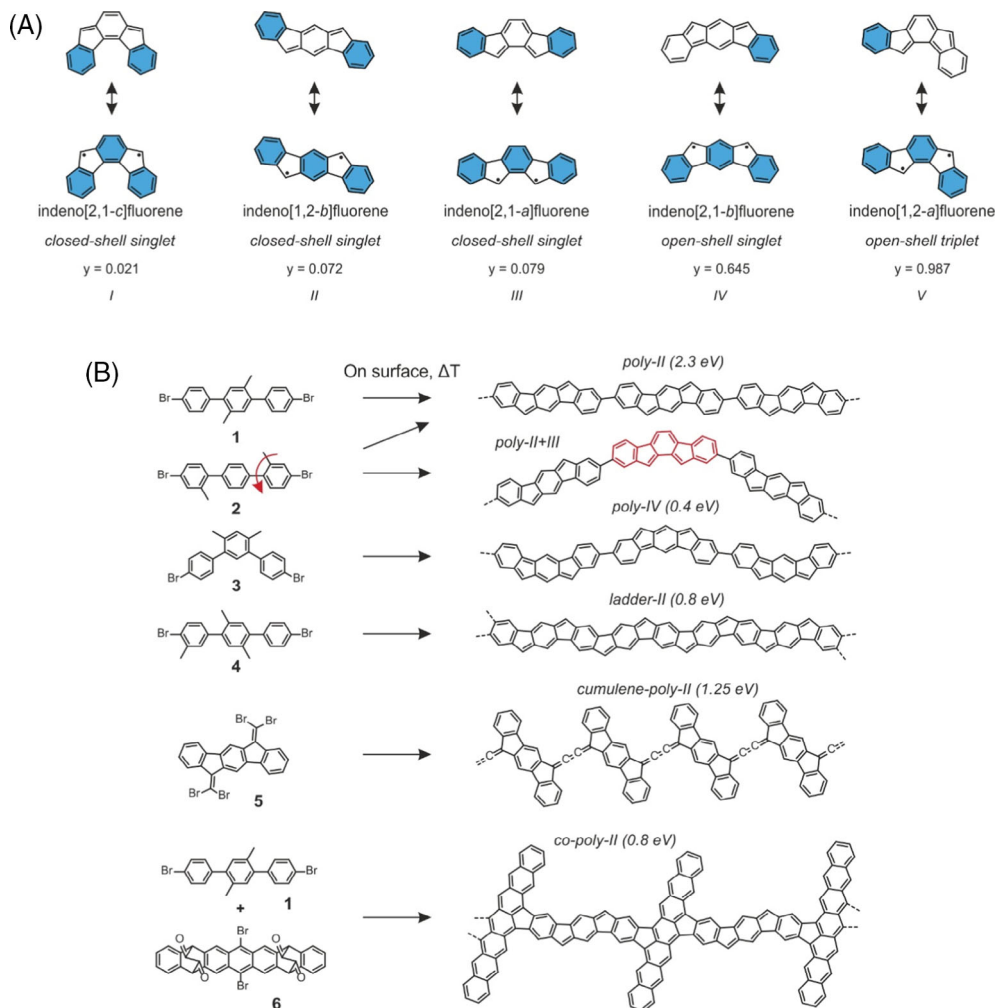
1 correspond to pure closed-shell and pure biradical electronic configurations, respectively. The drastic change in biradical character from *I–III* to *IV–V* can qualitatively be explained with the different gain of one or two aromatic sextets (highlighted in blue in Scheme 1A) when passing from the closed-shell Kekulé to the open-shell non-Kekulé resonance structures. Therefore, these systems represent fascinating compounds that can be used to answer fundamental questions about radical molecules.

The intrinsic reactivity of IFs and their derivatives has challenged synthetic chemists to develop stable products in which the highly reactive sites—apexes of five-membered rings—have been successfully stabilized by protecting groups.[8–15] Based on experimental and theoretical studies, a deep understanding of the binding motifs and electronic structure of these elusive compounds has been provided.[6,16–22] They demonstrated how radical character can be reconciled with chemical stability, and identified ground states and thermally accessible excited states of particular interest for magnetic switches in spintronics. They also described the optical properties and aromaticity patterns of IFs and related compounds,

as well as their behavior when incorporated in electronic devices (e.g., OFETs).

The fundamental appeal of IFs goes along with the application prospect of IF polymers—that is, extended, covalently linked chains consisting of IF units as monomeric building blocks. The synthesis of such materials is more challenging, as solubility and processability issues of large macromolecules add to the limitation of chemical stability. Nevertheless, successful results were achieved in 1991 by the seminal works of Scherf and Müllen,[23,24] which reported the formation of ladder-type polymers according to a polymer-analogous Friedel-Crafts cyclization after the formation of suitable polyphenylene backbones. These pioneering studies opened new avenues for the preparation of other ladder-type polymers.[25] Such materials were regarded as promising electroluminescent candidates for blue-light emission, together with step-ladder-type polymers obtained via a Yamamoto-type polymerization, which incorporate IF units linked together via single C—C bonds.[26–29] IF polymers where the repeat units are linked together at the five-membered rings of the IF scaffold were also reported, and their nonlinear

optical properties characterized.[30,31] IF copolymers were synthesized with the aim of improving light emission performance for OLEDs, engineering a suitable band gap for photovoltaic applications, and to enrich the *n*-channel semiconductor library.[32–36] However, synthesis of IF polymers (and monomers) always required suitable protecting groups and, to the best of our knowledge, there are no examples of unprotected IF polymers obtained via synthetic chemistry in solution.

An alternative, extremely powerful and versatile method for producing elusive compounds that would be unstable under ambient conditions is on-surface synthesis (OSS).[37,38] This approach uses carefully designed molecular precursors deposited on atomically flat substrates that serve as support, template and catalyst.[39–44] Specifically engineered functional groups in the molecular scaffold are activated via heat, radiation, or voltage to enable intra- and/or intermolecular chemical reactions, including covalent interconnections into polymers. The use of atomically flat substrates permits the application of atomically resolved characterization tools to study reaction intermediates and products, such as scanning tunneling microscopy/spectroscopy (STM/STS) and non-contact atomic force microscopy (nc-AFM). Performing experiments in ultrahigh vacuum (UHV) and studying samples at low temperature (at ~4 K) enables state-of-the-art imaging and tip functionalization (e.g., with single CO molecules) to resolve single atoms/bonds.[45]

Widely exploited—and well-controlled—strategies to grow low-dimensional carbon nanostructures on surfaces rely on the use of aryl halides as precursor molecules. Metal surface-catalyzed removal of the halogen atoms promotes dehalogenative aryl-aryl coupling between the molecular building blocks, thus affording one- or two-dimensional covalent chains or networks, depending on the halogen substitution pattern.[46–55] Polymerization can be followed by other chemical reactions, such as cyclodehydrogenation which plays an important role in the planarization of polyphenylenes to graphene nanoribbons (GNRs).[56–62] Fine tuning of such nanomaterials can be achieved by careful design and proper functionalization of the building blocks. In this regard, methyl groups have emerged as a promising functionality. First used for completing the zigzag edge of six-atom-wide zigzag-GNRs in 2016,[58] they have since been widely applied to the formation of both six-[62–67] and seven-membered[68,69] rings in various OSS protocols. In some case, loss of a methyl group inadvertently led to the formation of a pentagonal ring within an all-benzenoid framework,[65,70,71] but more importantly, methyl groups were also used to selectively form five-membered rings, as in the IF polymers described here or in indacenoditetracenes.[72]

Importantly, the reported methodology allowed to achieve unprotected IF units and thus to probe the electronic properties of IF polymers without perturbations from bulky protecting groups. This is possible due to the stabilization of the reactive radical compounds by the substrate and due to the absence of passivating agents under UHV conditions. Already before the OSS of unprotected IF polymers, unprotected IF monomers were achieved via STM tip-induced hydrogen cleavage from stable (closed-shell) dihydro-precursors.[73] Specifically, indeno[1,2-*b*]fluorene (*II*) was characterized on different substrates, which revealed an antiaromatic, closed-shell configuration when adsorbed on two monolayers of NaCl and deviations from a pure closed-shell configuration on Cu(111)—which highlighted the pivotal role of molecule-substrate interactions in determining the electronic ground state of such compounds.[73]

In this short review, we describe the recent successful on-surface growth of different types of unprotected, fully conjugated IF polymers (Scheme 1B), their structural characterization via high-resolution STM and bond-resolved nc-AFM imaging, and the insights obtained on their electronic properties via STS complemented by density-functional theory (DFT) calculations. All IF systems were achieved on clean Au(111) surfaces in UHV conditions upon thermal activation of the precursors depicted in the left side of Scheme 1B. Most of the reaction sequences started with an initial dehalogenative aryl-aryl coupling step, followed by oxidative methyl cyclization to afford five-membered rings on a polyphenylene backbone. Depending on precursor design, this resulted in step-ladder- or ladder-type IF polymers, which extended in the direction of the long axis of their IF constituents.[7,74,75] In another study, bromoethylene functional groups located at the five-membered ring apexes of an IF precursor afforded IF polymers that extended perpendicular to the long axis of their repeat units, with cumulene-like bridges between them.[76] Finally, IF precursors were also used as linkers to overcome steric hindrance in aryl-aryl homocoupling.[77] After an overview on all these results, we will discuss present challenges and future perspectives of IF polymers.

2 | INDENOFLUORENE POLYMERS

2.1 | Poly-II and poly-II + III

To synthesize IF polymers on surfaces, dibromo-terphenyl precursors equipped with methyl groups were used. Such molecular design entails several advantages: (i) the bromine substitutions at 4,4″ positions readily allow
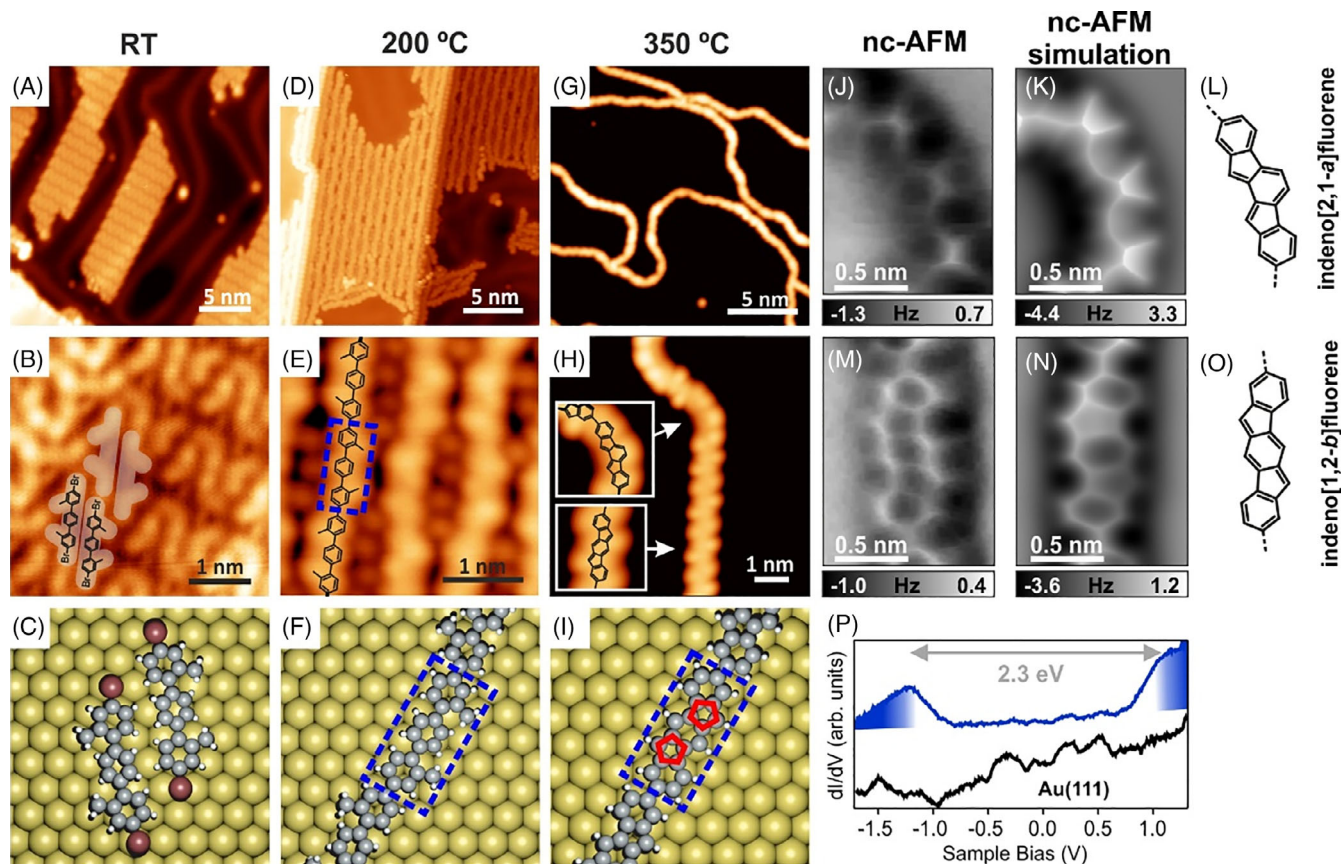
FIGURE 1 On-surface synthesis of *poly-II+III* from precursor **2**. STM images (A,B,D,E,G,H) and DFT optimized geometries (C,F,I) of precursor **2** deposited on Au(111) at RT and after annealing to the indicated temperatures. Constant-height frequency-shift nc-AFM images acquired with CO-functionalized tip at polymer segments consisting of unit *III* (J) and *II* (M), together with the simulated nc-AFM images (K,N) of the structures in panels (L,O). (P) Constant-height differential conductance (d*I*/d*V*) measurements performed on a straight segment—representative of *poly-II*—and on the bare substrate. Reproduced with permission.[74] Copyright 2018, American Chemical Society

for the formation of poly-phenylenes upon dehalogenative aryl-aryl coupling; (ii) anchoring the external phenylenes to the central one in *para* or *meta* positions enables the formation of poly-*para*- or poly-*meta*-phenylenes; (iii) the number and position of methyl groups dictate how many five-membered rings are formed via methyl cyclization along the poly-phenylene chain and also determine their spatial arrangement. These simple design tools open up a variety of combinations that lead to different IF polymers. Starting from the linear *para*-terphenyl backbone, installation of methyl groups at the 2′,5′ positions would lead to the formation of five-membered rings at opposite sides of the molecule, thus affording an indeno[1,2-*b*]fluorene unit (*II* in Scheme 1A). A 4,4″-dibromo-2′,5′-dimethyl-1,1′:4′,1″-terphenyl (**1**) precursor is then expected to afford *poly-II* (Scheme 1B). A more intriguing option is to anchor the methyl groups at the 2,2″ positions, as in the 4,4″-dibromo-2,2″-dimethyl-1,1′:4′,1″-terphenyl precursor (**2** in Scheme 1B), as the rotational freedom of the phenylene rings can in principle lead to two different final products.

The first example of unprotected IF polymers reported on surfaces indeed exploited precursor **2**.[74] After deposition on a clean Au(111) surface in UHV at room temperature (RT), the pristine compound assembled into islands of close-packed molecules, arranged in a back-to-back configuration (Figure 1A–C). The ease of rotation around the σ-bonds between phenylenes leads to an adsorption conformation where each molecule presents both methyl groups on the same side of its backbone. Although the two adsorption geometries—with methyl groups pointing in the same or in opposite directions with respect to the molecular backbone—are energetically equivalent for isolated species, DFT calculations reveal that, when two molecules are close to each other, the conformation with methyl groups on the same side is preferred by 0.1 eV, justifying the experimentally observed motif, which is most likely stabilized by halogen–hydrogen interactions.

After annealing the sample to 200 °C, one-dimensional polymers poly-**2** were obtained (Figure 1D–F), as confirmed by STM and XPS investigations. The spherical features observed between the polymers are assigned to

bromine atoms detached from the molecular precursors and chemisorbed on the Au(111) surface. In fact, the dissociation temperature of C—Br bonds on Au(111) was reported to be around 150 °C, and bromine desorption from this substrate around 250 °C, in agreement with other works.[78] The STM images clearly reveal that the methyl groups are still intact at this temperature, and that they point to the same side of the polymer chain in pairs (Figure 1E,F), indicating that no rotation around the molecular axis has occurred upon polymerization.

Bromine desorption and significant modifications in the appearance of the polymeric chains were reported after annealing to 350 °C (Figure 1G). Polymers are no longer packed in islands, as for poly-**2**, but meandering across the surface, with oligomer lengths up to 60 nm. Straight polymer segments consist of indeno[1,2-*b*]fluorene repeat units *II*, as unambiguously determined via nc-AFM imaging with a CO-functionalized tip, complemented by DFT simulations of the expected nc-AFM appearance (Figure 1H,I,M–O). The curved segments, forming angles of 25° and 60° with respect to a straight chain, arise from connection of two indeno[1,2-*b*]fluorene units (*II* in Scheme 1A) with opposite 2D chirality and from the presence of an indeno[2,1-*a*]fluorene unit (*III* in Scheme 1A) sandwiched between indeno[1,2-*b*]fluorene ones, respectively (Figure 1H,J–L). Constant-height nc-AFM imaging of such—minority—units *III* was less straightforward to interpret than of units *II* because of their non-planar geometry, which could, however, be resolved with height-dependent nc-AFM imaging. DFT calculations for an oligomer of *III* on Au(111) revealed a tilt of about 12° of its monomeric units with respect to the surface plane. Such non-planarity, attributed to an increased interaction of the radical sites at the five-membered ring apexes with the surface, is absent for type *II* units where the five-membered ring apexes are located at opposite sides and thus balance the overall interaction with the underlying substrate.

Considering the conformation of the monomeric units in the intermediate poly-**2**, with both methyl groups pointing to the same side, it is interesting to note that the final product after methyl cyclization consists predominantly of units *II* rather than *III*. Formation of *II* implies a rotation of an *ortho*-methyl substituted phenylene ring of poly-**2**, for which nudged elastic band DFT calculations predict an energy barrier of 0.7 eV.[79] This energy barrier can readily be overcome at the temperatures >300 °C used to achieve *poly-II+III*. On the other hand, direct cyclization of methyl groups from poly-**2** affords units *III*, but implies major geometrical rearrangements of the entire polymer chain to accommodate the in-plane curvature of

60° induced by the formation of *III*. In a classical transition state theory picture, such rearrangement is an event with significantly lower attempt frequency than the rotation of a phenylene ring, qualitatively explaining why units *II* are the main observed product in *poly-II+III*.

STS investigation of the final polymer on its straight segments—representative of *poly-II*—revealed a band gap of 2.3 eV on Au(111) (Figure 1P), in good agreement with the image charge corrected[80] quasiparticle GW gap of 2.0 eV calculated in gas phase.[81] The moderate biradical character of *II* compared to other IF isomers (Scheme 1A) was found to result in a closed-shell electronic ground state configuration of *poly-II*.

2.2 | Poly-IV

After the successful OSS of *poly-II+III* from a brominated terphenyl precursor equipped with two methyl groups, the next target was a polymer consisting of IF units with higher biradical character, that is, *IV* or *V* in Scheme 1A. The reason that these compounds exhibit $y > 0.5$ is qualitatively due to the increased gain of aromatic π-sextets (+2) from their closed- to the open-shell resonance structure, compared with only one in compounds *I–III*. A polymer containing the more symmetrical compound *IV* was targeted, to avoid potentially complex scenarios with the different 2D enantiomers of the prochiral compound *V*.

The precursor 4,4″-dibromo-4′,6′-dimethyl-1,1′:3′,1″-terphenyl (**3**) was designed to afford *poly-IV* via OSS on Au(111) (see Scheme 1B).[7] Upon deposition on the Au(111) surface held at RT, **3** adsorbed intact and formed self-assembled molecular islands stabilized by halogen-hydrogen interactions. Individual molecules could be manipulated away from an island with the STM tip and structurally characterized by STM and nc-AFM (Figure 2A,B). Such characterization confirmed the expected features for the intact precursor **3**, namely a twisted terphenyl molecular backbone, bromine atoms at the periphery, and bulky methyl groups protruding beyond the rest of the molecule.

After annealing to 150 °C, close-packed islands of zigzag chains were observed, with spherical protrusions between the chains that are attributed to bromine atoms detached from the precursor molecules and chemisorbed on the gold substrate, as discussed in the previous section (Figure 2C,D). The STM appearance of the chains matches the one expected for poly-**3** obtained from dehalogenative aryl-aryl coupling of **3**. Few polymer segments display consecutive *syn* bonding between repeat units that produces curved chains or closed loops, but the vast majority exhibit the characteristic zigzag profile
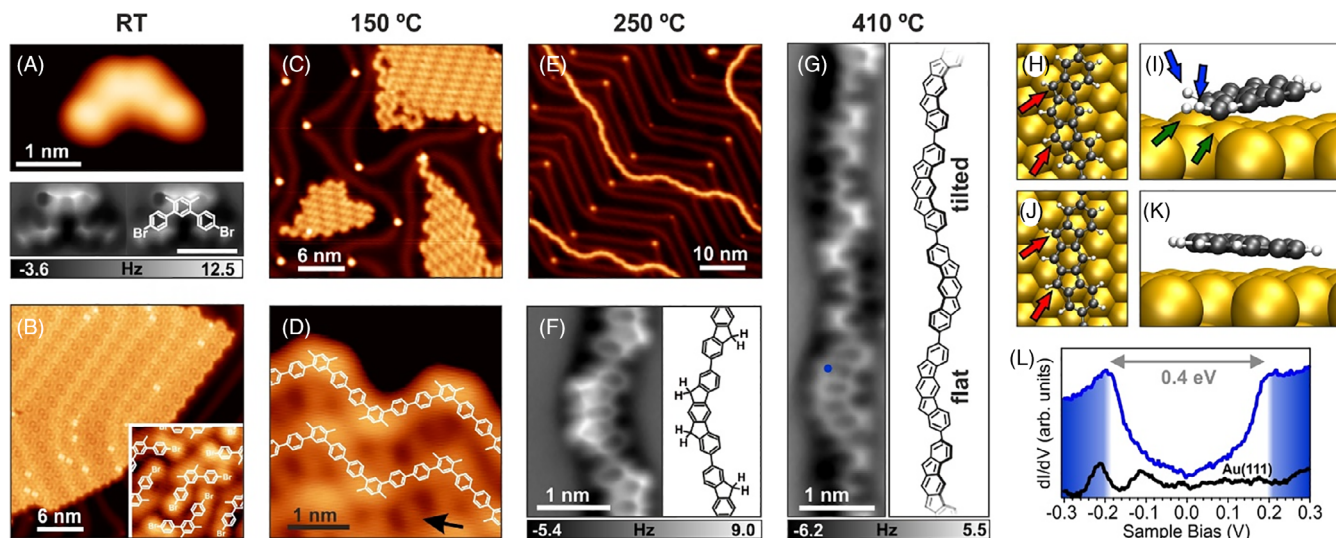
FIGURE 2 On-surface synthesis of *poly-IV* from precursor **3**. (A–E) STM images of precursor **3** deposited on Au(111) at RT, and after annealing to the indicated temperatures. Constant-height frequency-shift nc-AFM image acquired with CO-functionalized tip of an isolated molecule **3** (A), hydrogenated *poly-IV* (F), and *poly-IV* (G), with corresponding chemical schemes. DFT optimized geometries of oligomers where the carbon atoms at the apexes of five-membered rings (red arrows) lie on top of Au atoms (H,I) or on hollow sites (J,K). (L) Constant-height differential conductance (d*I*/d*V*) measurements performed on a flat unit of *poly-IV* and on the bare substrate. Reproduced with permission.[7] Copyright 2019, American Chemical Society

arising from *anti*-type linkages. Methyl groups appeared very similar to the ones of **3** after RT deposition, thus suggesting that they did not cyclize yet.

Bromine desorption—manifested by restoration of the Au(111) (22 × √3) herringbone surface reconstruction—and unpacking of the polymer islands were observed after annealing at 250 °C (Figure 2E). Constant-height frequency-shift nc-AFM imaging of the obtained polymers using a CO-functionalized tip revealed their chemical structure: Methyl groups have undergone oxidative cyclization and formed five-membered rings at the expected positions, but with brighter protrusions at their apexes which indicate the presence of doubly hydrogenated (sp^3) carbon atoms.[58,73] Hence, polymers consisting of 10,12-dihydroindeno[2,1-*b*]fluorene units were obtained at this stage.

To promote the desired further dehydrogenation step into *poly-IV*, annealing to 410 °C was performed. The resulting structural changes in the polymer chains could be clearly identified by STM and nc-AFM imaging (Figure 2G). Both flat (coplanar to the underlying surface) and tilted IF units were observed. The flat units showed no bright protrusions at the apexes of five-membered rings, confirming that the CH$_2$ functionalities were transformed into CH and the desired indeno[2,1-*b*]fluorene units (*IV* in Scheme 1A) were successfully achieved. The difference between flat and tilted IF units *IV* was explained in terms of their registry with respect to the underlying substrate surface. For the tilted units, carbon

atoms at the five-membered ring apexes lay on top of gold surface atoms (Figure 2H), which increases the interaction between that specific molecular unit and the surface and induces a tilt of the molecular plane (Figure 2I). In absence of such specific registry, the molecular units remain flat (Figure 2J,K). This scenario was confirmed by extensive DFT calculations taking into account various molecule-substrate registries. These also revealed that the tilted units induce a slight upward displacement of the involved Au atoms (green arrows in Figure 2I) and exhibit an out-of-plane bending of the C—H bond at the five-membered ring apexes (blue arrows in Figure 2I), witnessing an increased molecule-substrate interaction toward a chemisorption-like behavior.

STS investigation of *poly-IV* on Au(111) revealed a narrow band gap of 0.4 eV, strongly reduced from the value of 3.7 eV measured for the dihydro-species. Such energy gap is significantly lower than the value of 2.3 eV observed for *poly-II* on Au(111), which reflects the difference between the calculated HOMO-LUMO gaps of isolated species *IV* and *II* (1.23 and 1.97 eV, respectively).[5,12] Although frontier states in the d*I*/d*V* spectrum were found to be energetically symmetric around zero—a feature usually observed in case of spin (and other inelastic) excitations—different appearance of their d*I*/d*V* maps ruled out their possible origin from singly occupied orbitals. Even if STS measurements were conducted on the flat units of *poly-IV*, interaction with the underlying gold surface is apparently strong enough to quench the

expected biradical character of *IV*. High reactivity of *poly-IV* even under cleanest conditions such as in UHV was additionally witnessed by the frequent formation of porous ribbons arising from the lateral fusion of two *poly-IV* chains with face-to-face indeno[2,1-*b*]fluorene units, as detailed in the original work.[7]

Although the OSS of *poly-IV* did not lead to detection of the expected open-shell character on Au(111), theoretical investigations revealed appealing properties. DFT calculations at the (U)B3LYP/6-311G** level of theory for a short *oligo-IV* (pentamer) in gas phase predicted an open-shell singlet ground state with spin densities mainly located at the apexes of five-membered rings, as expected from Clar's theory. Moreover, the five-membered rings of such pentamer were found to be as antiaromatic as those of monomer *IV*, demonstrating that the polymer retained the aromaticity properties of the isolated units. Similar outcome was found for the biradical character, indicating that elongation of the structure into a polymer with σ-bond connectivity between repeat units does not alter the fundamental electronic properties of indeno[2,1-*b*]fluorene. Although the computed pentamer in gas phase presented a twist of ±35° between consecutive units, the same results obtained for a trimer with dihedral angle set to zero (i.e., flat units) suggested that planarization of *poly-IV* induced by adsorption on a substrate surface does not alter its electronic properties. The lack of experimental evidence for open-shell character in the experiments described above is therefore not due to the specific conformation of the adsorbed polymer, but rather to the strong chemical interaction between the highly reactive radical sites of *poly-IV* and the underlying gold surface, which acts similarly to passivating chemical agents.

2.3 | Ladder oligomers

The IF polymers discussed so far were "stepladder"-type chains, where doubly stranded segments (the IF units), representing ladder sections, are interconnected via single C—C bonds, the steps. Eliminating the steps and achieving ladder polymers—an uninterrupted sequence of rings with adjacent rings sharing two or more atoms[82]—would bring many benefits, but also presents quite a challenge. Absence of torsional motion around single bonds imparts rigidity and coplanarity to ladder polymers, resulting in improved thermal and mechanical stability as well as increased charge delocalization.[83,84] Conjugated ladder polymers promise high charge carrier mobility,[85,86] long exciton diffusion length,[87] and low energy gaps.[88,89] Synthesis of unprotected ladder polymers should be readily possible on surfaces, and the only

additional requirement compared to the previous cases of stepladder polymers is the addition of another methyl group at the precursor to create a five-membered ring at the position of the steps.

The 4,4″-dibromo-2′,3,5′-trimethyl-1,1′:4′,1″-terphenyl precursor (**4**) was employed in an attempt at the OSS of the corresponding *ladder-II* (Scheme 1B).[75] However, rotational freedom of the phenylene units prevented selectivity and resulted only in short oligomers of the desired structure, as we will discuss below. When deposited on Au(111) at RT, **4** assembled into molecular islands stabilized by halogen-hydrogen interactions (Figure 3A,B). Annealing of such sample to 160 °C triggered the formation of linear polymers via dehalogenative aryl-aryl coupling, as in the cases discussed above. Appearance of the backbone was unaltered as compared to the precursor molecules, indicating that the methyl groups had not yet reacted (Figure 3C,D).

However, annealing at 360 °C resulted in remarkable changes in polymer structure and assembly (Figure 3E). The resulting polymer chains were irregular, and composed of differently shaped parts. Nc-AFM imaging using a CO-functionalized tip revealed that most of the methyl groups had successfully cyclized into five-membered rings and formed the targeted methine bridges. However, many defects were revealed, such as (i) single C—C connections, (ii) methylene bridges, and (iii) two five-membered rings at the same chain site. These defects were attributed to (i) methyl cleavage or tail-to-tail connectivity of the precursors, (ii) incomplete dehydrogenation, and (iii) head-to-head coupling, respectively. The latter observation is of general interest as it suggests that aryl-aryl coupling may proceed even with two methyl groups at *ortho* positions.

Due to the large number of defects at random positions along the chains, only short defect-free segments whose length did not exceed 3 nm were observed (Figure 3G–J). In such segments, regular alternation of six and five-membered rings—with the latter pointing to opposite sides of the chain according to a *para* connection to the central six-membered ring—was successfully achieved. In other segments, absence of consecutive alternation of methyl groups before cyclization led to constitutional isomers with *meta* connections. Although relatively short, the regular segments of the obtained ladder polymer were found to be electronically equivalent to the targeted fully periodic IF ladder polymer. Indeed, STS characterization of such segments revealed d*I*/d*V* frontier orbital maps in agreement with the orbitals computed for the fully periodic IF ladder polymer, and a band gap of 0.8 eV on Au(111) (Figure 3F). DFT calculations revealed that the methine created from methyl groups had significant contribution to the conduction band (CB) and part of the valence band (VB), while the six-membered rings mainly contributed to the CB + 1 and
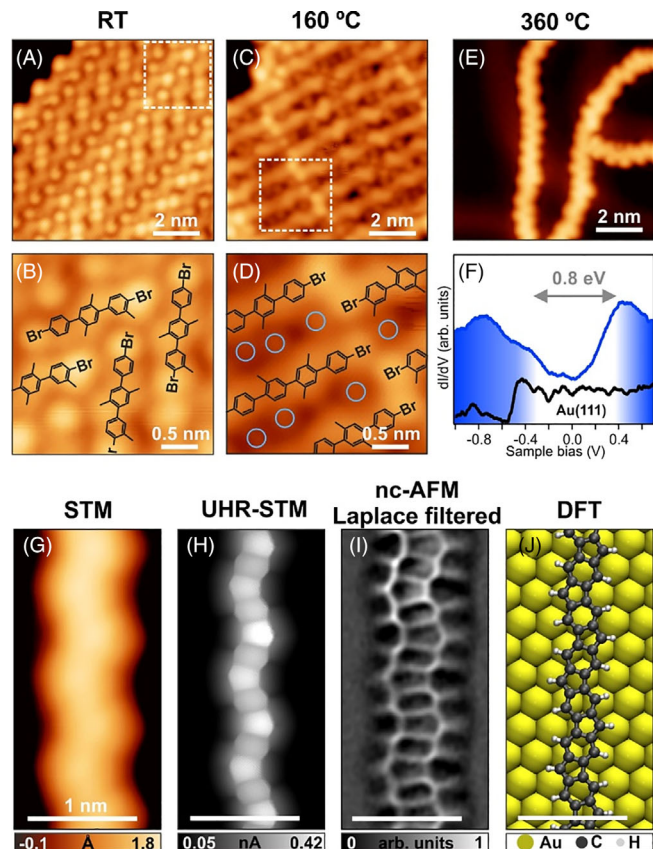
FIGURE 3 On-surface synthesis of *ladder-II* polymer from precursor **4**. (A–E) STM images of precursor **4** deposited on Au(111) at RT and after annealing to the indicated temperatures. (F) Constant-height differential conductance (dI/dV) measurements on a defect-free polymer segment and on the bare substrate. Defect-free ladder oligomer imaged via constant-current STM (G), and constant-height STM and nc-AFM with CO-functionalized tip (H,I). (J) DFT optimized geometry of the ladder polymer on Au(111). Reproduced with permission.[75] Copyright 2020, American Chemical Society

part of the VB, thus highlighting the role of the five-membered rings in achieving a low band gap. Interestingly, DFT also revealed that an infinite IF ladder polymer in gas phase is spin-polarized, with spin density largely localized at the five-membered ring apexes and an antiferromagnetic coupling between consecutive 5-membered rings.

2.4 | Cumulene-bridged indenofluorene polymers

In all examples of on-surface synthesized IF polymers discussed so far, the synthetic pathway relied on dehalogenative aryl-aryl coupling followed by methyl cyclization, resulting in polymer chain growth along the long axis of the molecular building blocks. An alternative on-surface synthetic protocol based on dibromomethylene

functional groups was reported to afford polymerization via cumulene bridges between five-membered ring apexes.[76] Installation of dibromomethylene groups at the apexes of five-membered rings of an indeno[1,2-*b*] fluorene unit was shown to protect the reactive sites of the precursor molecule and to afford polymers that extend perpendicularly to the long axis of their building blocks. A 6,12-bis(dibromomethylene)-6,12-dihydroindeno[1,2-*b*] fluorene precursor (**5**), obtained from an indeno[1,2-*b*] fluorene-6,12-dione via solution synthesis, was employed on Au(111) to grow *cumulene-poly-II* (Scheme 1B).[76] Although the reactive apexes of five-membered rings in these polymers are protected by the presence of connections between repeat units, this case has been included in the present review because of its interesting findings in terms of favored electronic configuration.

Precursor **5** was deposited on an Au(111) surface held at RT and subsequently annealed to 200 °C, which led to the formation of one-dimensional chains surrounded by dot-like features, attributed to bromine atoms chemisorbed on the gold surface (Figure 4A). The chemical structure of the obtained chains was characterized via nc-AFM imaging with CO-functionalized tip (Figure 4B,C), revealing intact indeno[1,2-*b*]fluorene scaffolds (*II* in Scheme 1A) and a cumulene-like linking motif between the repeat units. Electronic characterization by means of STS determined a band gap of 1.25 eV on Au(111) and a closed-shell electronic configuration.

The observation of a cumulene bridge between IF units is significant because it is directly related to the electronic configuration of the polymer. Two of the three possible resonance structures (Figure 4E) involve the presence of ethynylene bridges, with either closed- or open-shell configuration, similarly to the case of *II* in Scheme 1A. However, *II* exhibits very limited biradical character, and if the *cumulene-poly-II* behave similarly, they can be expected to adopt a closed-shell ground state configuration as well. The two closed-shell resonance structures illustrated in Figure 4E involve ethynylene and cumulene bridges, and contain two and three Clar sextets, respectively. Therefore, the cumulene-bridged closed-shell structure is expected to be preferred due to the higher number of stabilizing Clar sextets, and indeed it was the experimentally observed one. We note that these *cumulene-poly-II* could also be obtained from **5** on Ag(111) and Ag(100) at RT, where the activation of dibromomethylene groups occurs at lower temperature than on Au(111).[90]

2.5 | Indenofluorenes in copolymers

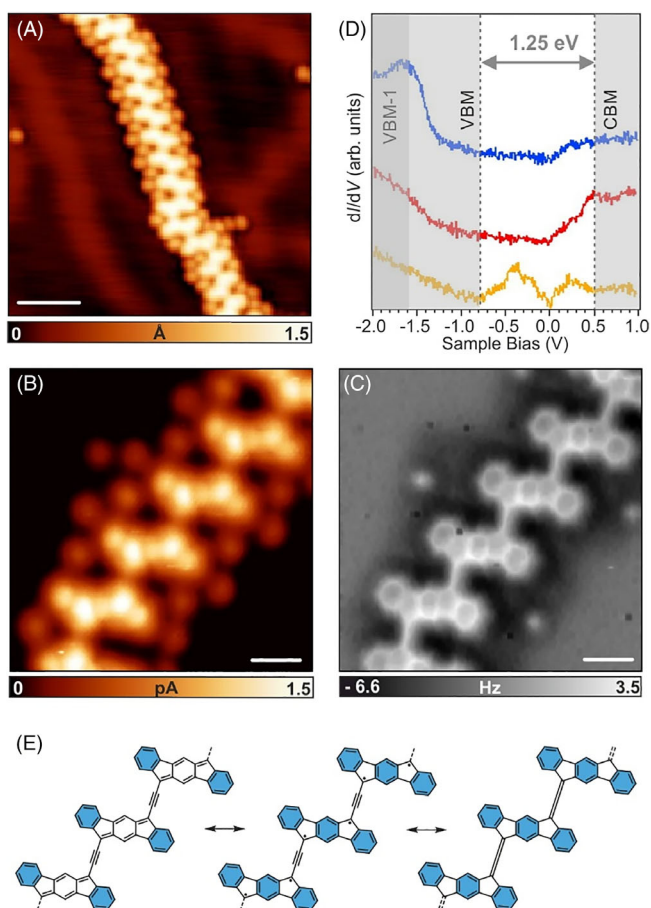In the introduction, the synthesis of IF copolymers has been motivated by the tuning of electronic properties

FIGURE 4 Growth of *cumulene-poly-II* from precursor **5**. Constant-current (A) and constant-height (B) STM images of precursor **4** after deposition on Au(111) at RT and subsequent annealing to 200 °C. (C) Constant-height frequency-shift nc-AFM image with CO-functionalized tip of a polymer segment. (D) Constant-height differential conductance (d*I*/d*V*) spectra of the *cumulene-bridged* polymer (blue and red curves) and bare Au(111) substrate (yellow curve). (E) Scheme of the possible resonance structures of the *cumulene-bridged* polymer involving ethynylene (left and center) and cumulene (right) bridges, with Clar sextets highlighted in blue. Reproduced with permission.[76] Copyright 2021, Royal Society of Chemistry

with respect to specific applications. Here, a different use of IFs in copolymers is presented, namely as linkers to overcome steric hindrance limitations in aryl-aryl coupling on surfaces. The underlying concept is rather straightforward and deals with numerous coupling issues observed in OSS. Contrary to solution-based methods, chemical reactions confined on surfaces suffer from reduced conformational freedom of the adsorbed reactants. Due to the energy gain resulting from van der Waals interaction with the substrate, molecules cannot explore all orientations and conformations they might have in the gas phase or in solution, and planar

geometries are usually preferred. However, such planarity may prevent intermolecular bond formation at the relevant reaction sites. As an example, activated heptacenes that would readily undergo aryl-aryl coupling at their 15, 18 radical sites in solution or in the gas phase cannot couple on a surface due to the steric repulsion of the neighboring hydrogen atoms which are coplanar to the radical sites (Figure 5A). This behavior was experimentally observed in several cases, leading to alternative products such as hydrogenated species,[77,91] organometallic compounds,[91–93] or to intramolecular rearrangements.[94]

To prepare covalently-linked, conjugated polymers from building blocks (B) that cannot homocouple, an alternative strategy is to connect them via suitable linkers (L) to form -B-L-B-L-B-L- chains. This approach can be used to fabricate elusive nanostructures and tune their electronic properties according to the combination of B and L. Such strategy was reported for the OSS of heptacene-based polymers, where the linker was an IF unit.[77] Heptacene precursor **6** (Scheme 1B), unable to homocouple, was deposited on an Au(111) surface together with 4,4″-dibromo-2′,5′-dimethyl-1,1′:4′,1″-terphenyl (**1**). Annealing such sample to 270 °C promoted dehalogenation of both precursors, aryl-aryl coupling, cleavage of α-diketone moieties from **6**, and cyclization of methyl groups in **1** toward five-membered rings. The resulting copolymer exhibited STM features resembling heptacene units spaced by linear segments (Figure 5B,C), that coexisted with unreacted heptacene molecules. Detailed chemical identification was achieved via nc-AFM imaging with CO-functionalized tip (Figure 5D), and revealed that the copolymer indeed consisted of heptacene units (B) linked together via indeno[1,2-*b*] fluorene entities (L, molecule *II* in Scheme 1A). Interestingly, at the connection point between B and L, additional five-membered rings were discerned, due to further CH activation and ring closure that occurred at a similar temperature as the methyl cyclization.

In this copolymerization scheme, precursors used as linkers (L) must have a geometry that does not lead to steric hindrance in the formation of intermolecular bonds. This property may, however, also lead to L-homocoupling. In fact, the desired building block alternation -B-L-B-L-B-L- was not always achieved, and segments consisting of consecutive L units were also observed. In the experiments described, B and L were co-deposited in a stoichiometric ratio of 1.8:1, with an excess of B to balance the ease of L-homocoupling. This led to 78% of B being incorporated in copolymers, while the remaining ones were found as isolated species. 69% of the heptacenes in the copolymers were separated by only one IF linker (i.e., in the
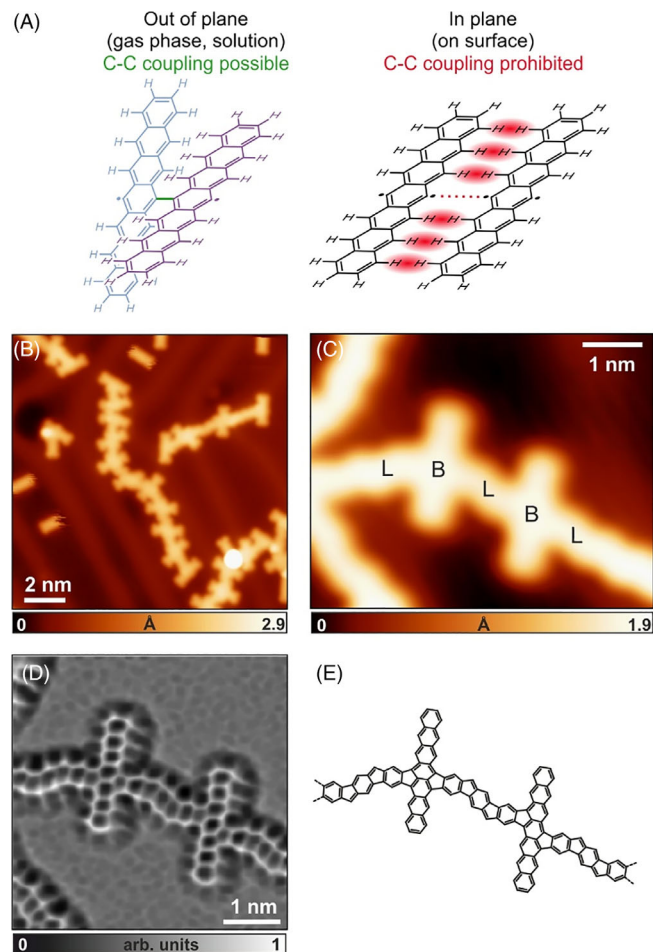
FIGURE 5 On-surface synthesis of *co-poly-II* from precursors **1** and **6**. (A) Scheme illustrating coupling issues on surfaces, as compared to solution-based processes. Activated heptacenes (e.g., from dibrominated compounds) can approach each other with a dihedral angle in solution or gas phase, which allows their covalent coupling (green bond). However, their planar adsorption geometry prevents similar coupling on a surface due to steric repulsion between hydrogen atoms (red areas) that keeps the active sites away from each other (red dotted line). (B, C) STM images of an Au(111) surface after deposition of **1** and **6** and annealing to 270 °C, with labeled alternation of building blocks (B) and IF linkers (L). (D) Constant-height frequency-shift nc-AFM image of a *copolymer* segment, revealing the chemical structure reported in E. reproduced with permission.[77] Copyright 2019, John Wiley and Sons

targeted -B-L-B-L-B-L- sequence), but the copolymer chains had a fairly short average length, with few chains reaching 20 nm or more. DFT calculations of the electronic properties of a regular copolymer segment adsorbed on Au(111) revealed a small band gap of 0.25 eV, strongly reduced from the values of *poly-II* (1.20 eV) and heptacene (0.50 eV). Energy gaps measured experimentally by STS confirmed this trend with values of 0.80 eV,[77] 2.30 eV,[74] and 1.50 eV[95] for the

copolymer, *poly-II*, and heptacene, respectively. The remarkably low band gap of the *copolymer* is due to the unusual, fully conjugated ladder-type nanowire structure achieved by using the IF linker **1**. Although it is imperative to further improve synthetic selectivity, these results clearly demonstrate the great potential of a copolymerization approach to tailor the structure and electronic properties of novel, complex nanomaterials.

3 | CONCLUSION

In this short review, an overview of recent progress in the on-surface synthesis of IF polymers has been reported. The appeal of IF-related compounds, which offer both a unique playground for the study of fundamental electronic properties and intriguing features for possible applications in organic electronics and spintronics, has led the OSS community to explore the fabrication of IF polymers. An important aspect of the reported results is that, unlike with solution-based methods, polymers with unprotected IF repeat units were obtained. This allowed the study of the electronic properties of pristine materials, that is, without stabilizing groups needed for solubility and processability in solution. Moreover, confinement of reactants and products on an atomically flat substrate in UHV allowed the study of reaction intermediates and final structures via scanning probe microscopies/spectroscopies, revealing subtle structural and electronic features that would have remained unexplored under different conditions.

The reported on-surface synthetic strategies rely on dehalogenative aryl-aryl coupling of dibromo-terphenyl precursors followed by the oxidative cyclization of methyl groups on the polyphenylene backbone to achieve the five-membered rings of the IF scaffolds. Alternative approaches where the molecular precursors featured the five-membered rings already before surface deposition required stabilization of the reactive sites—with extra hydrogen atoms[73] or dibromomethyl groups.[76] In the reported examples—except the case of *cumulene-poly-II*—the well-established dehalogenative aryl-aryl coupling step was thermally induced at 150 °C on Au(111). The methyl groups remained intact during this step and were activated at higher temperature for cyclization at the polyphenylene backbone. On Au(111) annealing to ~250 °C afforded cyclization and formation of methylene bridges, while heating at ~350 °C was needed to dehydrogenate the apexes of five-membered rings into methine bridges. This final step afforded the targeted, unprotected IF polymers.

Conjugated polymers consisting of different IF isomers and covering different biradical character values of the constituting units were obtained. The most

promising attempt to grow open-shell IF polymers was the case of *poly-IV*, since *IV* has a rather high biradical character index (Scheme 1). However, it was found that the polymers experienced a significant interaction with the underlying metal substrate, which induced a chemisorption-like behavior of the apexes of five-membered rings—the most reactive sites hosting unpaired electrons—and likely quenched any signature of their open-shell electronic configuration. This finding highlighted a long-standing limitation of OSS methods based on metal-catalyzed chemical reactions, i.e., the lack of adequate electronic decoupling of the on-surface synthesized compounds from the underlying metal. A possible solution could be the dry contact transfer of these reactive materials to more inert substrates under UHV conditions, which is being developed by several groups and will hopefully become routine for the scanning probe investigation of these and other unstable compounds in the near future.

ACKNOWLEDGMENTS

ORCID

Marco Di Giovannantonio https://orcid.org/0000-0001-8658-9183
Roman Fasel https://orcid.org/0000-0002-1553-6487

REFERENCES

[1] Z. Sun, Q. Ye, C. Chi, J. Wu, *Chem. Soc. Rev.* **2012**, *41*, 7857.
[2] A. Shimizu, S. Nobusue, H. Miyoshi, Y. Tobe, *Pure Appl. Chem.* **2014**, *86*, 517.
[3] Y. Tobe, *Chem. Rec.* **2015**, *15*, 86.
[4] T. Kubo, *Chem. Lett.* **2014**, *44*, 111.
[5] D. T. Chase, B. D. Rose, S. P. McClintock, L. N. Zakharov, M. M. Haley, *Angew. Chem., Int. Ed.* **2011**, *50*, 1127.
[6] K. Fukuda, T. Nagami, J. Fujiyoshi, M. Nakano, *J. Phys. Chem. A* **2015**, *119*, 10620.
[7] M. Di Giovannantonio, K. Eimre, A. V. Yakutovich, Q. Chen, S. Mishra, J. I. Urgel, C. A. Pignedoli, P. Ruffieux, K. Müllen, A. Narita, R. Fasel, *J. Am. Chem. Soc.* **2019**, *141*, 12346.
[8] G. E. Rudebusch, J. L. Zafra, K. Jorner, K. Fukuda, J. L. Marshall, I. Arrechea-Marcos, G. L. Espejo, R. Ponce Ortiz, C. J. Gómez-García, L. N. Zakharov, M. Nakano, H. Ottosson, J. Casado, M. M. Haley, *Nat. Chem.* **2016**, *8*, 753.
[9] A. Shimizu, Y. Tobe, *Angew. Chem., Int. Ed.* **2011**, *50*, 6906.
[10] D. T. Chase, A. G. Fix, S. J. Kang, B. D. Rose, C. D. Weber, Y. Zhong, L. N. Zakharov, M. C. Lonergan, C. Nuckolls, M. M. Haley, *J. Am. Chem. Soc.* **2012**, *134*, 10349.
[11] J. J. Dressler, Z. Zhou, J. L. Marshall, R. Kishi, S. Takamuku, Z. Wei, S. N. Spisak, M. Nakano, M. A. Petrukhina, M. M. Haley, *Am. Ethnol.* **2017**, *129*, 15565.
[12] A. Shimizu, R. Kishi, M. Nakano, D. Shiomi, K. Sato, T. Takui, I. Hisaki, M. Miyata, Y. Tobe, *Am. Ethnol.* **2013**, *125*, 6192.
[13] A. G. Fix, P. E. Deal, C. L. Vonnegut, B. D. Rose, L. N. Zakharov, M. M. Haley, *Org. Lett.* **2013**, *15*, 1362.
[14] J. J. Dressler, M. Teraoka, G. L. Espejo, R. Kishi, S. Takamuku, C. J. Gómez-García, L. N. Zakharov, M. Nakano, J. Casado, M. M. Haley, *Nat. Chem.* **2018**, *10*, 1134.
[15] C. Poriel, J. Rault-Berthelot, *Acc. Chem. Res.* **2018**, *51*, 1818.
[16] S. Thomas, K. S. Kim, *Phys. Chem. Chem. Phys.* **2014**, *16*, 24592.
[17] C. K. Frederickson, B. D. Rose, M. M. Haley, *Acc. Chem. Res.* **2017**, *50*, 977.
[18] G. E. Rudebusch, G. L. Espejo, J. L. Zafra, M. Peña-Alvarez, S. N. Spisak, K. Fukuda, Z. Wei, M. Nakano, M. A. Petrukhina, J. Casado, M. M. Haley, *J. Am. Chem. Soc.* **2016**, *138*, 12648.
[19] B. D. Rose, N. J. Sumner, A. S. Filatov, S. J. Peters, L. N. Zakharov, M. A. Petrukhina, M. M. Haley, *J. Am. Chem. Soc.* **2014**, *136*, 9181.
[20] M. R. Rao, A. Desmecht, D. F. Perepichka, *Chem. Eur. J.* **2015**, *21*, 6193.
[21] A. M. Zeidell, L. Jennings, C. K. Frederickson, Q. Ai, J. J. Dressler, L. N. Zakharov, C. Risko, M. M. Haley, O. D. Jurchescu, *Chem. Mater.* **2019**, *31*, 6962.
[22] H. Miyoshi, M. Miki, S. Hirano, A. Shimizu, R. Kishi, K. Fukuda, D. Shiomi, K. Sato, T. Takui, I. Hisaki, M. Nakano, Y. Tobe, *J. Org. Chem.* **2017**, *82*, 1380.
[23] U. Scherf, K. Müllen, *Makromol. Chem., Rapid Commun.* **1991**, *12*, 489.
[24] U. Scherf, K. Müllen, *Polymer* **1992**, *33*, 2443.
[25] U. Scherf, *J. Mater. Chem.* **1999**, *9*, 1853.
[26] S. Setayesh, D. Marsitzky, K. Müllen, *Macromolecules* **2000**, *33*, 2016.
[27] J. Jacob, J. Zhang, A. C. Grimsdale, K. Müllen, M. Gaal, E. J. W. List, *Macromolecules* **2003**, *36*, 8240.
[28] J. Jacob, S. Sax, T. Piok, E. J. W. List, A. C. Grimsdale, K. Müllen, *J. Am. Chem. Soc.* **2004**, *126*, 6987.
[29] A. C. Grimsdale, P. Leclère, R. Lazzaroni, J. D. MacKenzie, C. Murphy, S. Setayesh, C. Silva, R. H. Friend, K. Müllen, *Adv. Funct. Mater.* **2002**, *12*, 729.
[30] H. Reisch, U. Wiesler, U. Scherf, N. Tuytuylkov, *Macromolecules* **1996**, *29*, 8204.
[31] M. Samoc, A. Samoc, B. Luther-Davies, H. Reisch, U. Scherf, *Opt. Lett.* **1998**, *23*, 1295.
[32] D. Marsitzky, J. C. Scott, J.-P. Chen, V. Y. Lee, R. D. Miller, S. Setayesh, K. Müllen, *Adv. Mater.* **2001**, *13*, 1096.
[33] C. Duan, W. Cai, C. Zhong, Y. Li, X. Wang, F. Huang, Y. Cao, *J. Polym. Sci. Part Polym. Chem.* **2011**, *49*, 4406.
[34] H. Usta, A. Facchetti, T. J. Marks, *J. Am. Chem. Soc.* **2008**, *130*, 8580.
[35] H. Usta, C. Risko, Z. Wang, H. Huang, M. K. Deliomeroglu, A. Zhukhovitskiy, A. Facchetti, T. J. Marks, *J. Am. Chem. Soc.* **2009**, *131*, 5586.
[36] D. Mei, L. Yang, L. Zhao, S. Wang, H. Tian, J. Ding, L. Wang, *J. Mater. Chem. C* **2020**, *8*, 14819.
[37] S. Clair, D. G. de Oteyza, *Chem. Rev.* **2019**, *119*, 4717.
[38] L. Grill, S. Hecht, *Nat. Chem.* **2020**, *12*, 115.
[39] J. Sakamoto, J. van Heijst, O. Lukin, A. D. Schlüter, *Angew. Chem., Int. Ed.* **2009**, *48*, 1030.

[40] R. Lindner, A. Kühnle, *ChemPhysChem* **2015**, *16*, 1582.

[41] M. Lackinger, *Chem. Commun.* **2017**, *53*, 7872.

[42] Q. Shen, H.-Y. Gao, H. Fuchs, *Nano Today* **2017**, *13*, 77.

[43] D. G. de Oteyza, C. Rogero Eds., *On-Surface Synthesis II: Proceedings of the International Workshop On-Surface Synthesis, San Sebastián, 27–30 June 2016*, Springer International Publishing, Cham **2018**.

[44] M. Di Giovannantonio, G. Contini, *J. Phys. Condens. Matter* **2018**, *30*, 093001.

[45] L. Gross, F. Mohn, N. Moll, P. Liljeroth, G. Meyer, *Science* **2009**, *325*, 1110.

[46] L. Grill, M. Dyer, L. Lafferentz, M. Persson, M. V. Peters, S. Hecht, *Nat. Nanotechnol.* **2007**, *2*, 687.

[47] J. A. Lipton-Duffin, O. Ivasenko, D. F. Perepichka, F. Rosei, *Small* **2009**, *5*, 592.

[48] M. Bieri, M.-T. Nguyen, O. Gröning, J. Cai, M. Treier, K. Aït-Mansour, P. Ruffieux, C. A. Pignedoli, D. Passerone, M. Kastler, K. Müllen, R. Fasel, *J. Am. Chem. Soc.* **2010**, *132*, 16669.

[49] M. Bieri, S. Blankenburg, M. Kivala, C. A. Pignedoli, P. Ruffieux, K. Müllen, R. Fasel, *Chem. Commun.* **2011**, *47*, 10239.

[50] L. Lafferentz, V. Eberhardt, C. Dri, C. Africh, G. Comelli, F. Esch, S. Hecht, L. Grill, *Nat. Chem.* **2012**, *4*, 215.

[51] M. Di Giovannantonio, M. El Garah, J. Lipton-Duffin, V. Meunier, L. Cardenas, Y. Fagot Revurat, A. Cossaro, A. Verdini, D. F. Perepichka, F. Rosei, G. Contini, *ACS Nano* **2013**, *7*, 8190.

[52] J. Eichhorn, D. Nieckarz, O. Ochs, D. Samanta, M. Schmittel, P. J. Szabelski, M. Lackinger, *ACS Nano* **2014**, *8*, 7880.

[53] G. Vasseur, Y. Fagot-Revurat, M. Sicot, B. Kierren, L. Moreau, D. Malterre, L. Cardenas, G. Galeotti, J. Lipton-Duffin, F. Rosei, M. Di Giovannantonio, G. Contini, P. Le Fèvre, F. Bertran, L. Liang, V. Meunier, D. F. Perepichka, *Nat. Commun.* **2016**, *7*, 10235.

[54] C. Moreno, M. Vilas-Varela, B. Kretz, A. Garcia-Lekue, M. V. Costache, M. Paradinas, M. Panighel, G. Ceballos, S. O. Valenzuela, D. Peña, A. Mugarza, *Science* **2018**, *360*, 199.

[55] G. Galeotti, F. De Marchi, E. Hamzehpoor, O. MacLean, M. Rajeswara Rao, Y. Chen, L. V. Besteiro, D. Dettmann, L. Ferrari, F. Frezza, P. M. Sheverdyaeva, R. Liu, A. K. Kundu, P. Moras, M. Ebrahimi, M. C. Gallagher, F. Rosei, D. F. Perepichka, G. Contini, *Nat. Mater.* **2020**, *19*, 874.

[56] J. Cai, P. Ruffieux, R. Jaafar, M. Bieri, T. Braun, S. Blankenburg, M. Muoth, A. P. Seitsonen, M. Saleh, X. Feng, K. Müllen, R. Fasel, *Nature* **2010**, *466*, 470.

[57] P. Ruffieux, J. Cai, N. C. Plumb, L. Patthey, D. Prezzi, A. Ferretti, E. Molinari, X. Feng, K. Müllen, C. A. Pignedoli, R. Fasel, *ACS Nano* **2012**, *6*, 6930.

[58] P. Ruffieux, S. Wang, B. Yang, C. Sánchez-Sánchez, J. Liu, T. Dienel, L. Talirz, P. Shinde, C. A. Pignedoli, D. Passerone, T. Dumslaff, X. Feng, K. Müllen, R. Fasel, *Nature* **2016**, *531*, 489.

[59] L. Talirz, H. Söde, T. Dumslaff, S. Wang, J. R. Sanchez-Valencia, J. Liu, P. Shinde, C. A. Pignedoli, L. Liang, V. Meunier, N. C. Plumb, M. Shi, X. Feng, A. Narita, K. Müllen, R. Fasel, P. Ruffieux, *ACS Nano* **2017**, *11*, 1380.

[60] L. Talirz, P. Ruffieux, R. Fasel, *Adv. Mater.* **2016**, *28*, 6222.

[61] D. G. de Oteyza, A. García-Lekue, M. Vilas-Varela, N. Merino-Díez, E. Carbonell-Sanromà, M. Corso, G. Vasseur, C. Rogero, E. Guitián, J. I. Pascual, J. E. Ortega, Y. Wakayama, D. Peña, *ACS Nano* **2016**, *10*, 9000.

[62] O. Gröning, S. Wang, X. Yao, C. A. Pignedoli, G. Borin Barin, C. Daniels, A. Cupo, V. Meunier, X. Feng, A. Narita, K. Müllen, P. Ruffieux, R. Fasel, *Nature* **2018**, *560*, 209.

[63] S. Mishra, D. Beyer, K. Eimre, J. Liu, R. Berger, O. Gröning, C. A. Pignedoli, K. Müllen, R. Fasel, X. Feng, P. Ruffieux, *J. Am. Chem. Soc.* **2019**, *141*, 10621.

[64] S. Mishra, D. Beyer, K. Eimre, S. Kezilebieke, R. Berger, O. Gröning, C. A. Pignedoli, K. Müllen, P. Liljeroth, P. Ruffieux, X. Feng, R. Fasel, *Nat. Nanotechnol.* **2020**, *15*, 22.

[65] S. Mishra, D. Beyer, R. Berger, J. Liu, O. Groening, J. I. Urgel, K. Müllen, P. Ruffieux, X. Feng, R. Fasel, *J. Am. Chem. Soc.* **2020**, *142*, 1147.

[66] Q. Sun, L. M. Mateo, R. Robles, P. Ruffieux, N. Lorente, G. Bottari, T. Torres, R. Fasel, *J. Am. Chem. Soc.* **2020**, *142*, 18109.

[67] X. Su, C. Li, Q. Du, K. Tao, S. Wang, P. Yu, *Nano Lett.* **2020**, *20*, 6859.

[68] S. Mishra, T. G. Lohr, C. A. Pignedoli, J. Liu, R. Berger, J. I. Urgel, K. Müllen, X. Feng, P. Ruffieux, R. Fasel, *ACS Nano* **2018**, *12*, 11917.

[69] T. G. Lohr, J. I. Urgel, K. Eimre, J. Liu, M. Di Giovannantonio, S. Mishra, R. Berger, P. Ruffieux, C. A. Pignedoli, R. Fasel, X. Feng, *J. Am. Chem. Soc.* **2020**, *142*, 13565.

[70] Y. Zheng, C. Li, Y. Zhao, D. Beyer, G. Wang, C. Xu, X. Yue, Y. Chen, D.-D. Guan, Y.-Y. Li, H. Zheng, C. Liu, W. Luo, X. Feng, S. Wang, J. Jia, *Phys. Rev. Lett.* **2020**, *124*, 147206.

[71] X. Xu, M. Di Giovannantonio, J. I. Urgel, C. A. Pignedoli, P. Ruffieux, K. Müllen, R. Fasel, A. Narita, *Nano Res.* **2021**, *14*, 4754.

[72] R. Zuzak, O. Stoica, R. Blieck, A. M. Echavarren, S. Godlewski, *ACS Nano* **2021**, *15*, 1548.

[73] Z. Majzik, N. Pavliček, M. Vilas-Varela, D. Pérez, N. Moll, E. Guitián, G. Meyer, D. Peña, L. Gross, *Nat. Commun.* **2018**, *9*, 1198.

[74] M. Di Giovannantonio, J. I. Urgel, U. Beser, A. V. Yakutovich, J. Wilhelm, C. A. Pignedoli, P. Ruffieux, A. Narita, K. Müllen, R. Fasel, *J. Am. Chem. Soc.* **2018**, *140*, 3532.

[75] M. Di Giovannantonio, Q. Chen, J. I. Urgel, P. Ruffieux, C. A. Pignedoli, K. Müllen, A. Narita, R. Fasel, *J. Am. Chem. Soc.* **2020**, *142*, 12925.

[76] C. Martín-Fuentes, J. I. Urgel, S. Edalatmanesh, E. Rodríguez-Sánchez, J. Santos, P. Mutombo, K. Biswas, K. Lauwaet, J. M. Gallego, R. Miranda, P. Jelínek, N. Martín, D. Écija, *Chem. Commun.* **2021**, *57*, 7545.

[77] J. I. Urgel, M. Di Giovannantonio, G. Gandus, Q. Chen, X. Liu, H. Hayashi, P. Ruffieux, S. Decurtins, A. Narita, D. Passerone, H. Yamada, S.-X. Liu, K. Müllen, C. A. Pignedoli, R. Fasel, *ChemPhysChem* **2019**, *20*, 2360.

[78] M. Di Giovannantonio, O. Deniz, J. I. Urgel, R. Widmer, T. Dienel, S. Stolz, C. Sánchez-Sánchez, M. Muntwiler, T. Dumslaff, R. Berger, A. Narita, X. Feng, K. Müllen, P. Ruffieux, R. Fasel, *ACS Nano* **2018**, *12*, 74.

[79] G. Henkelman, B. P. Uberuaga, H. Jónsson, *J. Chem. Phys.* **2000**, *113*, 9901.

[80] J. B. Neaton, M. S. Hybertsen, S. G. Louie, *Phys. Rev. Lett.* **2006**, *97*, 216405.

[81] J. Wilhelm, M. Del Ben, J. Hutter, *J. Chem. Theory Comput.* **2016**, *12*, 3623.

[82] *Compendium of polymer terminology and nomenclature*; **2009**.

[83] C. Zhu, A. J. Kalin, L. Fang, *Acc. Chem. Res.* **2019**, *52*, 1089.

[84] J. Lee, A. J. Kalin, T. Yuan, M. Al-Hashimi, L. Fang, *Chem. Sci.* **2017**, *8*, 2503.

[85] P. Prins, F. C. Grozema, J. M. Schins, S. Patil, U. Scherf, L. D. A. Siebbeles, *Phys. Rev. Lett.* **2006**, *96*, 146601.

[86] A. Babel, S. A. Jenekhe, *J. Am. Chem. Soc.* **2003**, *125*, 13656.

[87] M. Samiullah, D. Moghe, U. Scherf, S. Guha, *Phys. Rev. B* **2010**, *82*, 205211.

[88] M. Kertesz, T. R. Hughbanks, *Synth. Met.* **1995**, *69*, 699.

[89] A. Tsuda, A. Osuka, *Science* **2001**, *293*, 79.

[90] M. Fritton, D. A. Duncan, P. S. Deimel, A. Rastgoo-Lahrood, F. Allegretti, J. V. Barth, W. M. Heckl, J. Björk, M. Lackinger, *J. Am. Chem. Soc.* **2019**, *141*, 4824.

[91] J. I. Urgel, H. Hayashi, M. Di Giovannantonio, C. A. Pignedoli, S. Mishra, O. Deniz, M. Yamashita, T. Dienel, P. Ruffieux, H. Yamada, R. Fasel, *J. Am. Chem. Soc.* **2017**, *139*, 11658.

[92] A. Basagni, L. Ferrighi, M. Cattelan, L. Nicolas, K. Handrup, L. Vaghi, A. Papagni, F. Sedona, C. D. Valentin, S. Agnoli, M. Sambi, *Chem. Commun.* **2015**, *51*, 12593.

[93] J. Park, K. Y. Kim, K.-H. Chung, J. K. Yoon, H. Kim, S. Han, S.-J. Kahng, *J. Phys. Chem. C* **2011**, *115*, 14834.

[94] F. Eisenhut, T. Lehmann, A. Viertel, D. Skidin, J. Krüger, S. Nikipar, D. A. Ryndyk, C. Joachim, S. Hecht, F. Moresco, G. Cuniberti, *ACS Nano* **2017**, *11*, 12419.

[95] J. I. Urgel, S. Mishra, H. Hayashi, J. Wilhelm, C. A. Pignedoli, M. Di Giovannantonio, R. Widmer, M. Yamashita, N. Hieda, P. Ruffieux, H. Yamada, R. Fasel, *Nat. Commun.* **2019**, *10*, 861.

AUTHOR BIOGRAPHIES

Marco Di Giovannantonio received his Master in Material Science and Technology (2011) and PhD in Physics (2015) from University of Rome "Tor Vergata", Italy. In 2016 he joined the nanotech@surfaces Laboratory of Prof. Dr. Roman Fasel at Empa (Switzerland) as postdoctoral research fellow until 2019, and as scientist until 2020. In 2020 he was enrolled by the Italian National Research Council (CNR) and since then he works as scientist at the Institute of Structure of Matter (ISM) in Rome, Italy. His research interests focus on surface-confined chemical reactions to achieve novel functional nanomaterials.

Roman Fasel obtained his PhD in Physics in 1996 from the University of Fribourg (Switzerland). He is the head of the nanotech@surfaces Laboratory of Empa, the Swiss Federal Laboratories for Materials Science and Technology, and adjunct professor at the Department of Chemistry of the University of Bern. His research covers a wide range of topics at the interface of materials science, surface physics and chemistry. With his team he has pioneered the on-surface synthesis of graphene nanoribbons which yields atomically precise nanoribbon structures with widely tunable (opto)electronic properties.